Journal of Computational and Applied Mechanics, Vol. 7., No. 1., (2006), pp. 85–101

INDUSTRIAL ROBOT APPLIED IN NEUROREHABILITATION [Arm and shoulder exercising by robot]

András Tóth, Gustáv Arz, László L. Kovács, Gábor Stépán
Budapest University of Technology and Economics
Műegytem rkp. 3-5., H-1521 Budapest, Hungary
{toth|arz}@manuf.bme.hu, {kovacs|stepan}mm.bme.hu

Gábor Fazekas
National Institute for Medical Rehabilitation
Szanatórium utca 19., H-1528 Budakeszi, Hungary
kassai@alarmix.net

[Received: August 31, 2004]

Abstract. This paper reports the latest results of the REHAROB IST-1999-13109 project. The objectives of the project; the structure of the REHAROB Therapeutic System, and the architecture of the applied teaching in force controller are presented. The paper also describes the results of the first clinical trial with the REHAROB Therapeutic System. The results proved that using industrial robots for passive motion therapy is a promising approach to improving motor deficit after stroke.

Keywords: stroke, neurorehabilitation, industrial robots, teaching in, force control

1. Introduction

A characteristic neurological impairment of stroke patients is the spastic hemiparesis of the limbs. Annual incidence of stroke is between 150 and 400 cases for each 100000 population in the European Union while it is 214 annual cases in the United States of America and 400 cases in Hungary [1]. Eighty percent of stroke survivors have significant neurological impairment. Sixty-nine percent of them can be rehabilitated successfully while the rest of the survivors need help in everyday activities. Evidence has shown that early and intensive motion therapy positively affects the restoration of the motor function after stroke [2]. Budget constraints, however, limit the realization of a labour-intensive, one-to-one, two times per day physiotherapy in the rehabilitation practice. Widely available Continuous Passive Motion (CPM) exercising machines used for post-surgical rehabilitation are not suitable for antispastic physiotherapy.

Research groups in the US, Asia, and Europe are attempting to develop robotic systems that would assist the physiotherapists in gait, trunk, balance, arm, hand, and finger rehabilitation of spastic hemiparetic patients. The ARM Guide [3], the MIME [4], the MIT-MANUS [5], ArmTrainer and the GENTLE/S [6] are the best known spastic arm physiotherapy systems. The MIT-MANUS has gained commercial

success with a few installations, whilst the others remain operational in the developers' rehabilitation organizations.

2. The REHAROB therapeutic system

The REHAROB Therapeutic System [7] (shown in Figure 1) was designed to bring advances in three fundamental features of robotic antispastic physiotherapy:

1. REHAROB uses two robotic manipulators for controlled moving of the upper arm and the lower arm of the patient
2. REHAROB performs complex full anatomic Range of Motion (ROM) exercises on all possible shoulder girdle and elbow motions: shoulder protraction-retraction, shoulder elevation-depression, shoulder flexion-extension, shoulder abduction-adduction, shoulder external-internal rotation, elbow flexion-extension, and lower arm pronation-supination
3. REHAROB was built from mass produced commercial components like industrial robots in order to cut product costs and to achieve critical mass for viable production

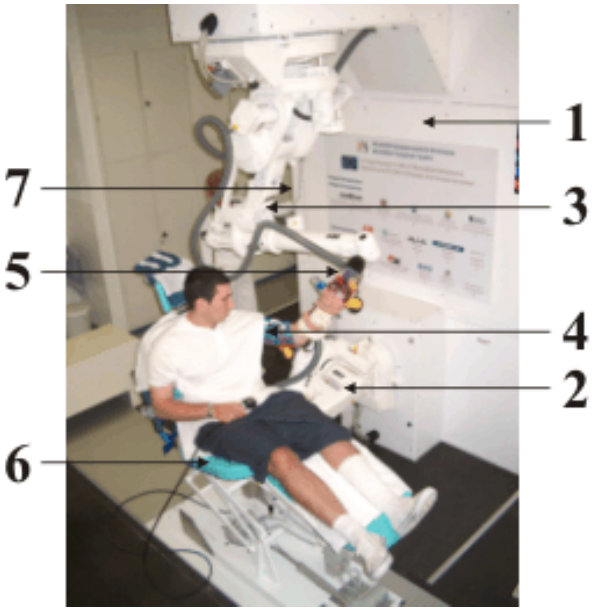

Figure 1. The REHAROB Therapeutic System: 1 Frame, 2 IRB 140 industrial robot, 3 IRB 1400H industrial robot, 4 Upper-arm orthosis, 5 Lower-arm orthosis, 6 Couch, and 7 Operating panel

Programming of the system is realized by demonstration of the exercises through force controlled industrial robots. For delivery of exercises to the patient two ABB industrial robots were selected: the wall mounted 0.8m reach IRB 140 industrial robot

is connected to the upper arm and the inverted 1.4m reach IRB 1400H industrial robot is connected to the lower arm. A powered turnable couch positions the patient according to the required treatment which can be lying or sitting, and left arm or right arm for any patient size. Mechanical design of the frame and the couch was completed so that REHAROB is fully symmetrical to left arm and right arm therapy.

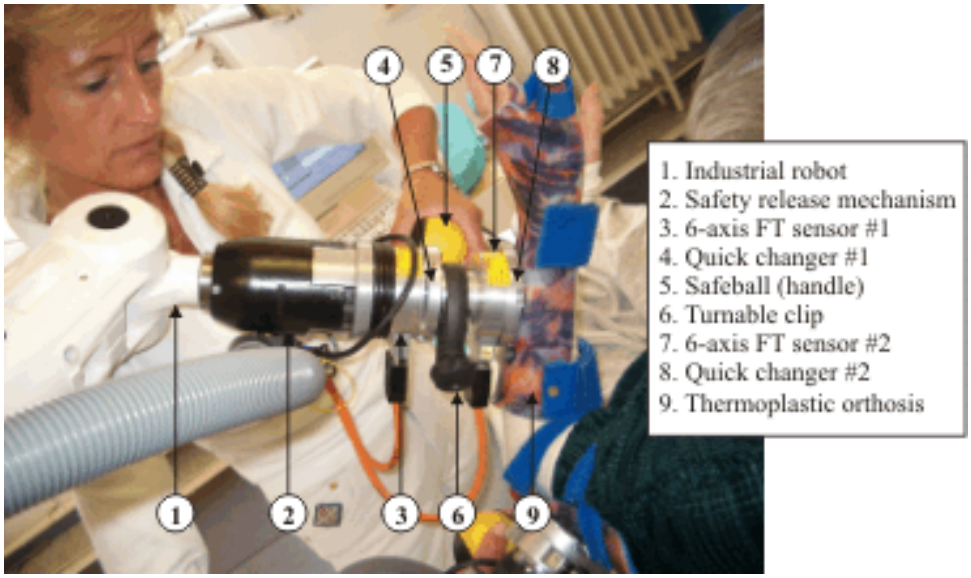

Figure 2. Teaching in of the physiotherapy exercises with the help of instrumented orthoses

The instrumented orthoses, which connect the patient's arm to the robots, include safety, control and coupling devices as follows (from left to right in Figure 2): Safety release mechanism, six DOF F/T sensor for force control, quick changer #1, safeball® with a turnable clip, six DOF F/T sensor for force monitoring, quick changer #2, three sized thermoplastic orthosis. The control system of REHAROB involves the two industrial robot controllers, the four sets of 6-axis force/torque measurement systems, the so-called watchdog PC and the high level controller PC. We have developed a novel outer-loop indirect force control method for programming the standard industrial robots [8]. This is called teaching in, during which the physiotherapist freely exercises the patient by leading the orthoses through the required trajectory with grasping the safeballs®, while the robots follow and learn the trajectories (see Figure 2). The operating devices and the user interface of the control system were designed not only for safety but also for the maximum comfort of the physiotherapist (PT). In addition to the control devices assembled on the orthoses and on the couch, there is an operating panel on the frame. The panel includes a Touch Screen Display, a keyboard, 3 buttons, and 3 switches only.

Figure 3. The operating panel and the user interface

Industrial robots, defined by the industrial robot safety standard EN ISO 8373:1994, must not be used in applications where contact with the human body can happen. The IRB 140 and the IRB 1400H industrial robots meet the requirements of 18 safety and harmonized standards (not listed here due to space limitations), which is a great advantage but does not make yet the system eligible for robotic physiotherapy. Special safety devices and monitoring programs were developed for, and tested with the robotic rehabilitation system. The REHAROB Therapeutic System is a medical device, so it meets fully the requirements of the relevant European directive, the Medical Device Directive [9].

3. Mechanical model of the teaching in device

The teaching in device of the robot is the part of the instrumented orthosis system. The main units of the device are: the safety release mechanism (SRM), the 6-axis FT sensor #1 and the safeball® as shown in Figure 4.

In the model presented the mass m_1 stands for the inertia of the SRM flange and half of the 6-xis FT sensor #1 (see Figure 2). The mass m_2 represents the mass of remaining part of the instrumented orthosis towards the patient's arm and also the mass of the patient's arm itself [10]. Stiffness s_1 is the effective stiffness of the elements located in the SRM, while s_2 denotes the stiffness of the FT sensor #1. The damping factors k_1 and k_2 model the small material damping of the helical springs of the SRM and the FT sensor #1, respectively. The dynamical parameters of the physiotherapist's hand are identified by stiffness s_3 and damping factor k_3.

In Figure 4 the coordinates x_1 and x_2 denote the positions of the center point of the FT sensor #1 and the safeball, respectively. The position of the robot is

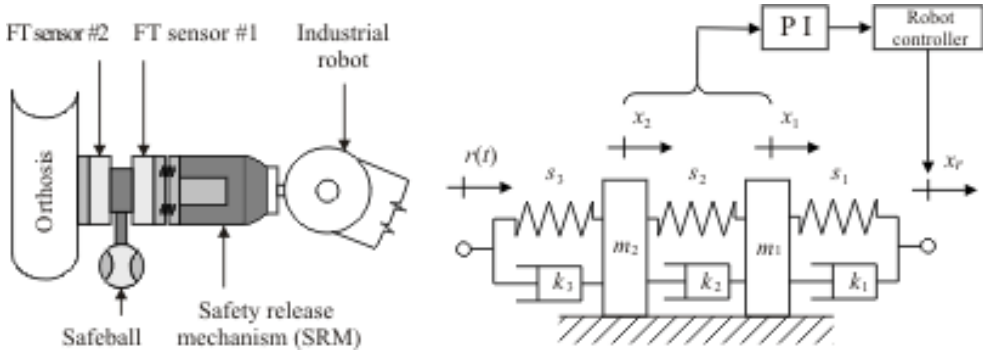

Figure 4. Mechanical model of the teaching in device

measured by the coordinate x_r and the physiotherapist's motion is described by the time dependent displacement function $r(t)$.

The equations of motion of the above one-dimensional mechanical model, i.e. the simplified model of the teaching in device, are as follows

$$\begin{aligned} m_1\ddot{x}_1 &= s_1\,(x_r - x_1) - s_2\,(x_2 - x_1) + k_1\,(\dot{x}_r - \dot{x}_1) - k_1\,(\dot{x}_r - \dot{x}_1) \\ m_2\ddot{x}_2 &= s_2\,(x_1 - x_2) - s_2\,(x_2 - r(t)) + k_2\,(\dot{x}_1 - \dot{x}_2) - k_1\,(\dot{x}_2 - \dot{r}(t)) \\ \dot{x}_r &= v_n \qquad t \in [t, t + \Delta t) \end{aligned} \tag{1}$$

where Δt is the controller's sampling time and v_n is the velocity of the robot for the actual sampling period. Then, using the notation $t_n = n\Delta t$ to denote time instants and introducing the state vector $\mathbf{x} = (x_1,\, x_2,\, \dot{x}_1,\, \dot{x}_2)$ the integration of the third equation in (1) yields the vector form

$$\dot{\mathbf{x}} = \mathbf{A}\mathbf{x} + [x_{r,n} + v_n(t - t_n)]\,\mathbf{b}_o + v_n\mathbf{b}_1 + \mathbf{u}(t)\;, \qquad t \in [t_n, t_{n+1})\;, \tag{2}$$

where the coefficient matrix $\mathbf{A}$ is

$$\begin{bmatrix} 0 & 0 & 1 & 0 \\ 0 & 0 & 0 & 1 \\ -\dfrac{s_1 + s_2}{m_1} & \dfrac{s_2}{m_1} & -\dfrac{k_1 + k_2}{m_1} & -\dfrac{k_2}{m_1} \\ \dfrac{s_2}{m_2} & -\dfrac{s_2 + s_3}{m_2} & \dfrac{k_2}{m_2} & -\dfrac{k_2 + k_3}{m_2} \end{bmatrix}\;, \tag{3}$$

and the non-homogeneous vector terms $\mathbf{b}_o$, $\mathbf{b}_1$ and $\mathbf{u}(t)$ are

$$\mathbf{b}_o = \begin{bmatrix} 0 \\ 0 \\ s_1/m_1 \\ 0 \end{bmatrix}\;,\quad \mathbf{b}_1 = \begin{bmatrix} 0 \\ 0 \\ k_1/m_1 \\ 0 \end{bmatrix}\;,\quad \mathbf{b}_o = \begin{bmatrix} 0 \\ 0 \\ 0 \\ r(t)\,s_3/m_2 + \dot{r}(t)\,k_3/m_2 \end{bmatrix}\;. \tag{4}$$

4. **Teaching in force control strategy**

The control strategy applied in REHAROB is defined as outer-loop or indirect force control in the literature [11]. The block scheme of the control is presented in Figure 5. Using this approach, the outer-loop force controller commands the position/orientation inputs to the robot controller. In this way, industrial robots become easily programmable by the technically not well-qualified physiotherapists.

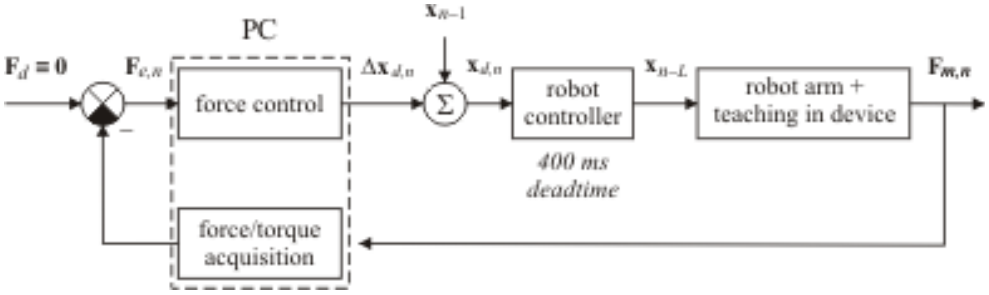

Figure 5. Outer-loop indirect force control

Figure 5 shows that the reference signal $\mathbf{F}_{e,n}$ of the outer-loop force controller is equal to the measured force $\mathbf{F}_{n,n}$ since the desired contact force $\mathbf{F}_d = 0$, or in other words, the robot is required to follow the physiotherapist's motion without any resistance. The outer-loop force controller commands the desired robot position/orientation $\mathbf{x}_{d,n}$ relative to the position $\mathbf{x}_{n-1}$ realized at the end of the previous sampling interval. In addition to the digital sampling effect, the control is also influenced by the 400 ms deadtime (confirmed by ABB) of the robot controller. This deadtime is modeled as the product of an integer L and the sampling time of the outer force control loop.

In REHAROB, the outer-loop force controller is integrated with the signal-processing unit of the 6-axis FT sensor. The commanded pose data are directly transferred to the robot using standard serial connection and the FT sensor can be sampled up to 1 kHz. However, due to the limitations in the communication speed (115 Kbit/s) and the limited number of executable motion instructions in a certain time period (approximately 65 instructions in a second) of the applied industrial robots, the feasible control frequency was found to be 10 Hz as a maximum.

The relatively low sampling frequency of the discrete time control and also the presence of the large deadtime in the system are against the stability of the outer force control loop. This also made it difficult to tune the parameters of the empirically derived PI control law

$$v_n = -K_p\,(x_{1,n-L} - x_{2,n-L}) - K_l \sum_{i=1}^{n} f_d^{n-j}\;(x_{1,j-L} - x_{2,j-L})\;\Delta t\;, \quad t \in [t_n\, t_{n+1}) \tag{5}$$

where K_p and K_l are the proportional and integral gains of the controller, respectively. In addition, $f_d < 1$ is the weight factor of the special integral term, which provides descending weights for the past values of the measured force, expressed here via the deformation $x_1 - x_2$ of FT sensor #1.

5. **Stability analysis**

The stability of the simplified, one-dimensional model (see Figure 4) is investigated by the solution of the equation of motion (2). It is assumed in the form

$$\mathbf{x} = \mathbf{x}_r^d + \boldsymbol{\xi} \tag{6}$$

where $\boldsymbol{\xi}$ is a small perturbation around the desired robot motion which satisfies equation (2). Thus, the asymptotic stability of the zero trivial solution of the corresponding variational system

$$\dot{\boldsymbol{\xi}} = \mathbf{A}\boldsymbol{\xi} + \left[\xi_{r,n} + \vartheta_n(t - t_n)\right]\mathbf{b}_o + \vartheta_n \mathbf{b}_1 \ , \quad t \in [t_n, t_{n+1}) \tag{7}$$

with the perturbed velocity

$$\vartheta_n = -K_p\left(\xi_{1,n-L} - \xi_{2,n-L}\right) - K_l \sum_{i=1}^{n} f_d^{n-j}\ \left(\xi_{1,j-L} - \xi_{2,j-L}\right)\ \Delta t \ , \quad t \in [t_n\, t_{n+1}) \tag{8}$$

refers to the realization of the desired robot motion and zero contact force. Note that the trajectory error corresponding to the error of the outer force control loop is a function of the control and mechanical parameters.

The stability investigation of the piecewise continuous system (7) is carried out via the analytical construction of a discrete mapping possessing the same stability properties [12]. In order to construct this mapping the following four-step algorithm is advised

1. The general solution of (7) has to be calculated for the interval.
2. The constant of the general solution has to be determined by the substitution of the initial condition into the general solution of (7).
3. The state variable has to be calculated at the end of the n^{th} sampling period.
4. Choosing an appropriate discrete state vector, it is practical to arrange the results in a dense matrix form.

According to the above algorithm, the stability of the trivial solution of (7) can be investigated by the convergence of the discrete mapping

$$\boldsymbol{\xi} = \mathbf{P}\boldsymbol{\xi}_n + \mathbf{Q}\mathbf{b}_o\vartheta_n + \mathbf{R}\mathbf{b}_o\boldsymbol{\xi}_{r,n} + \mathbf{R}\mathbf{b}_1\vartheta_n \tag{9}$$

where the corresponding coefficient matrices are

$$\begin{aligned} &\mathbf{P} = \exp\left(\mathbf{A}\Delta t\right) \ , \quad \mathbf{Q} = \exp\left(\mathbf{A}\Delta t\right)\mathbf{A}^{-2} - \mathbf{A}^{-2} - \mathbf{A}^{-1}\Delta t \ , \\ &\mathbf{R} = \exp\left(\mathbf{A}\Delta t\right)\mathbf{A}^{-1} - \mathbf{A}^{-2} \end{aligned} \tag{10}$$

In addition, the perturbed velocity (8) of the robot can be formulated as

$$\vartheta_n = -P\left(\xi_{1,n-L} - \xi_{2,n-L}\right) - I\xi_{int,n-L} \tag{11}$$

where $\xi_{int,n-L}$ is defined by the recursive formula

$$\xi_{int,n-L} = f_d\,\xi_{int,n-L-1} + (\xi_{1,n-L} - \xi_{2,n-L})\,\Delta t\ . \tag{12}$$

Applying the notation $\Delta\xi_n = \xi_{1,n} - \xi_{2,n}$ for the perturbed deformation of the FT sensor #1, the discrete mapping (9) can be expressed in the form

$$\mathbf{z}_{n+1} = \mathbf{D}\,\mathbf{z}_n \tag{13}$$

where the discrete state vector is

$$\mathbf{z}_n = \left[\xi_{r,n},\, \xi_{1,n},\, \xi_{2,n},\, \dot{\xi}_{1,n},\, \dot{\xi}_{2,n},\, \xi_{int,n-L-1},\, \Delta\xi_{n-L},\, \Delta\xi_{n-L+1}\,, \ldots, \Delta\xi_{n-1}\right]^T\ . \tag{14}$$

Finally, the so-called transition matrix has the form

$$\mathbf{D} = \begin{bmatrix}
1 & 0 & 0 & 0 & 0 & -\hat{K}_l\Delta t & -\hat{K}_p\Delta t & 0 & 0 & \cdots & 0 & 0 \\
R_{13}\frac{s_1}{m_1} & P_{11} & P_{12} & P_{13} & P_{14} & D_{26} & D_{27} & 0 & 0 & \cdots & 0 & 0 \\
R_{23}\frac{s_1}{m_1} & P_{21} & P_{22} & P_{23} & P_{24} & D_{36} & D_{37} & 0 & 0 & \cdots & 0 & 0 \\
R_{33}\frac{s_1}{m_1} & P_{31} & P_{32} & P_{33} & P_{34} & D_{46} & D_{47} & 0 & 0 & \cdots & 0 & 0 \\
R_{43}\frac{s_1}{m_1} & P_{41} & P_{42} & P_{43} & P_{44} & D_{56} & D_{57} & 0 & 0 & \cdots & 0 & 0 \\
0 & 0 & 0 & 0 & 0 & f_d & \Delta t & 0 & 0 & \cdots & 0 & 0 \\
0 & 0 & 0 & 0 & 0 & 0 & 0 & 1 & 0 & \cdots & 0 & 0 \\
0 & 0 & 0 & 0 & 0 & 0 & 0 & 0 & 1 & \cdots & 0 & 0 \\
0 & 0 & 0 & 0 & 0 & 0 & 0 & 0 & 0 & \cdots & 0 & 0 \\
\vdots & \vdots & \vdots & \vdots & \vdots & \vdots & \vdots & \vdots & \vdots & \ddots & \vdots & \vdots \\
0 & 0 & 0 & 0 & 0 & 0 & 0 & 0 & 0 & \cdots & 0 & 1 \\
0 & 1 & -1 & 0 & 0 & 0 & 0 & 0 & 0 & \cdots & 0 & 0
\end{bmatrix} \tag{15}$$

in which

$$D_{i6} = -\hat{K}_l\left(Q_{i-1,3}\frac{s_1}{m_1} + R_{i-1,3}\frac{k_1}{m_1}\right)\ ,\quad D_{i7} = -\hat{K}_p\left(Q_{i-1,3}\frac{s_1}{m_1} + R_{i-1,3}\frac{k_1}{m_1}\right)\ .$$
$$i = 2, \ldots, 5 \tag{16a}$$

The modified control gains $\hat{K}_p$ and $\hat{K}_l$ are defined by

$$\hat{K}_p = K_p + K_l\,\Delta t \qquad \text{and} \qquad \hat{K}_l = f_d\,K_l\ . \tag{16b}$$

Stability of the zero trivial solution of (7) is determined by the eigenvalues of the coefficient matrix (15). If all the eigenvalues μ_k $k = 1, 2, \ldots, L+6$ of the transition matrix $\mathbf{D}$ (the so-called characteristic multipliers) are located inside the open unit disc of the complex plane, then the system is asymptotically stable [12,13].

Taking into consideration the model parameters listed in Table 1 and Table 2, the corresponding stability chart is shown in Figure 6. The dynamic parameters of the physiotherapist's hand were estimated by simple experiments and intuition. These parameters can, naturally, vary in a certain range. Table 1 defines the range of the stiffness parameter between 2000 and 5000 N/m, while the corresponding damping factors are given to provide a realistic (relative) damping ratio of 80%.

Table 1. Mechanical parameters

Symbol	**Value**	**Symbol**	**Value**
m_1	0.1 [kg]	m_2	4 [kg]
s_1	15000 [N/m]	s_2	10^7 [N/m]
s_3	2000 ŧ 5000 [N/m]	k_1	1 [Ns/m]
k_1	1 [Ns/m]	k_2	143 – 226[Ns/m]

Table 2. Control parameters

Symbol	**Description**	**Value**
K_p	Proportional gain	4000 [1/s]
K_l	Integral gain	4000 [1/s^2]
f_d	Dissipation factor of the integral term	0.7 [-]
Δt	Sampling time	100 [ms]
L	Deadtime parameter	4 [-]

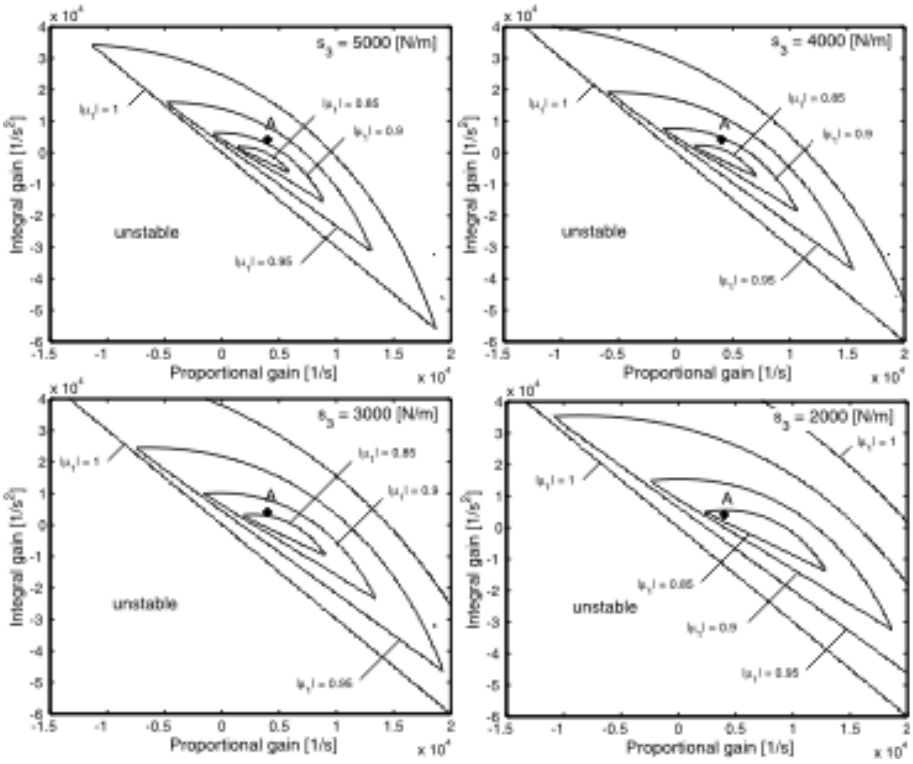

Figure 6. Stability chart of the control gains varying with stiffness s_3

The experimentally tuned gain parameters $K_p = 4000\,[1/s]$ and $K_f = 4000\,[1/s^2]$ are denoted by point A. This point is near the central region of each chart where the characteristic multiplier $|\mu_1| \leqslant 0.85$ is small enough to provide fast decaying control.

6. **Simulation and experimental results**

The stability charts presented in the previous section are calculated semi-analytically. These charts correspond to the simplified, one-dimensional mechanical model shown in Figure 4 with the measured and estimated mechanical and control parameters listed in Table 1 and Table 2, respectively. The accuracy of the charts presented was tested by simulation and experiments.

During the clinical test of REHAROB (see Section 5 for details) a large number of exercises were recorded. A typical taught in trajectory in one direction is presented in Figure 7.

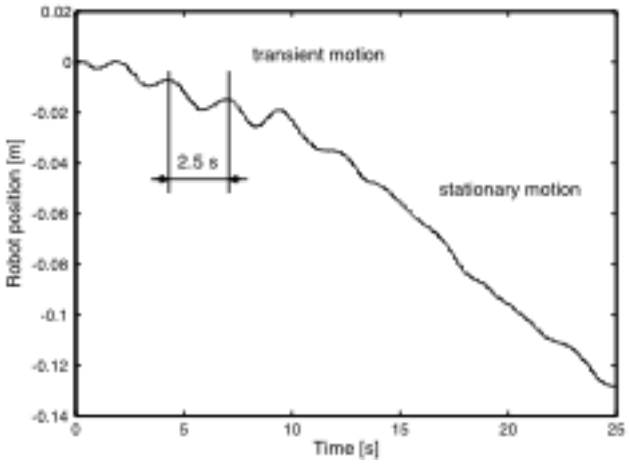

Figure 7. Measured robot trajectory

Figure 7 shows that each exercise segment starts with a transient because even a skilled physiotherapist cannot compensate completely for the deadtime during start of teaching in an exercise. The frequency of these transient vibrations can be estimated by

$$f = \frac{Im(\ln \mu_{A,1})}{2\pi\Delta t} = 0.422\ [\mathrm{Hz}]\,, \tag{17}$$

where $\mu_{A,1} = 0.8812 + 0.2393i$ is the largest characteristic multiplier at point A. The good agreement between this analytical result and the measured frequency 0.4 Hz of the transient motion presented in Figure 7 verifies the simplified, one-dimensional model and its parameters. The transient motion of the model was simulated by Simulink® Matlab®. The simplified block scheme of the Simulink® model is presented in Figure 8.

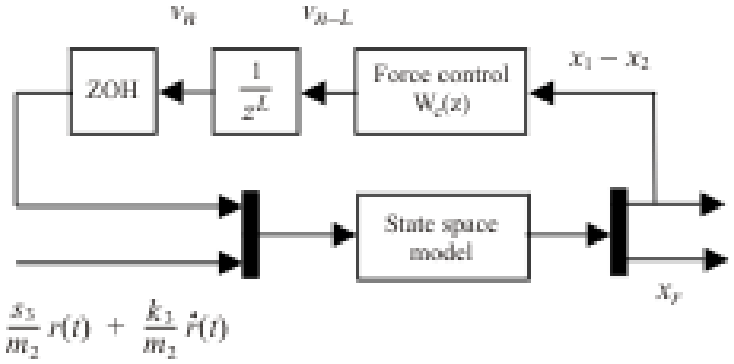

Figure 8. Simplified block scheme of the Simulink® model

In the simulation, the dynamics of the system was modeled by the state-space representation of (1) as follows

$$\begin{bmatrix} \dot{x}_r \\ \dot{\mathbf{x}} \end{bmatrix} = \left(\begin{bmatrix} 0 \\ \mathbf{b}_o \end{bmatrix} \begin{bmatrix} 1 & 0 & 0 & 0 & 0 \end{bmatrix} + \begin{bmatrix} 0 & \mathbf{0}^T \\ \mathbf{0} & \mathbf{A} \end{bmatrix} \right) \begin{bmatrix} x_r \\ \mathbf{x} \end{bmatrix} + \\ + \begin{bmatrix} 1 & 0 & 0 & 0 & 0 \\ 0 & 0 & 0 & 0 & 1 \end{bmatrix}^T \begin{bmatrix} v_n \\ \mathbf{u}(t) \end{bmatrix}, \quad (18)$$

$$\begin{bmatrix} x_1 - x_2 \\ x_r \end{bmatrix} = \begin{bmatrix} 0 & 1 & -1 & 0 & 0 \\ 1 & 0 & 0 & 0 & 0 \end{bmatrix} \begin{bmatrix} x_r \\ \mathbf{x} \end{bmatrix} + \begin{bmatrix} 0 & 0 \\ 0 & 0 \end{bmatrix} \begin{bmatrix} v_n \\ u(t) \end{bmatrix}. \quad (19)$$

According to the expression (5) of the control law, the outer-loop force controller has the impulse transfer function

$$W_c(z) = \frac{v_n(z)}{x_{1,n}(z) - x_{2,n}(z)} = \frac{-(K_P + K_I \Delta t)z + K_P f_d}{z - f_d}, \quad (20)$$

which transforms the impulse sequence of the sensor deformations $x_1 - x_2$ into the prescribed velocities at discrete time instants. The input $r(t)$, i.e. the motion that the physiotherapist would achieve, is generated from the measured robot trajectory presented in Figure 7. The desired motion is calculated by the 9^{th} order polynomial approximation of the measured data. The desired, simulated and measured robot trajectories are presented in Figure 9, which shows that the transient vibration in the simulated time history can be observed for the initial 2 seconds only, which is in contrast with the measurements. A possible explanation for this is that the mechanical and the control model of the physiotherapist is oversimplified. Note that in the one-dimensional model applied only the stiffness s_3 and the damping k_3 dynamic parameters represent the physiotherapist. However, the reflex delay of the physiotherapist shall also affect the system dynamics in a somewhat destabilizing way [14].

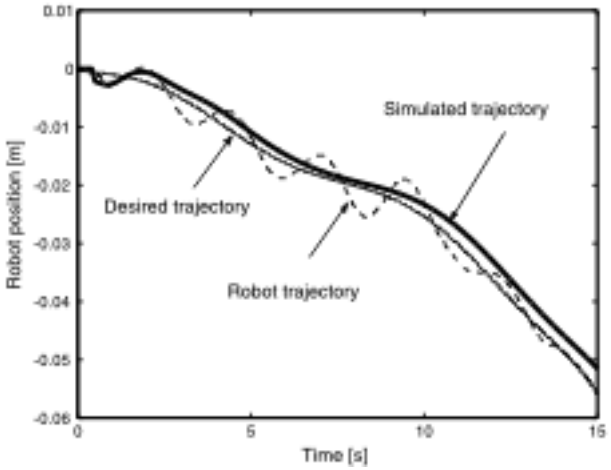

Figure 9. Desired, simulated and the measured robot trajectories

7. **Clinical testing**

The REHAROB Therapeutic System was installed in the National Institute for Medical Rehabilitation, Budapest, Hungary for clinical testing. It is very important to note that clinical testing is the formal part of medical certification, and its objective is not the study of the clinical efficiency but, as quoted to verify that, under normal conditions of use, the performance of the devices conform to those intended by the manufacturer, and to determine any undesirable side-effects, under normal conditions of use, and assess whether they constitute risks when weighed against the intended performance of the device. The clinical testing started on the 6^{th} of April 2003 with three healthy female and one male volunteers of age from 28 to 44. The second group and the third group of subjects included patients. The patient's clinical data are shown in Table 3. Each subject received 30 minutes net robotic physiotherapy, excluding sitting in- and out, and teaching in the exercises on 20 consecutive working days. After 7200 minutes total robotic physiotherapy the clinical trial ended on the 8^{th} of July 2003.

Table 3. Clinical data of the patients

Patient #	**Sex**	**Age**	**Diagnosis**	**Setting up**	**Hand affected**
R1	Male	71	Ischaemic stroke	9 years ago	Right
R2	Male	64	Ischaemic stroke	9 years ago	Right
R3	Male	26	Subdural haemorrhage	5 years ago	Right
R4	Female	56	Subarachnoideal haemorrhage	3 years ago	Right
R5	Female	66	Ischaemic stroke	5 weeks ago	Left
R6	Male	20	Epidural haemorrhage	9 months ago	Left
R7	Male	46	Basilar artery thrombosis	22 months ago	Right
R8	Male	25	Cavernoma pontis	8 weeks ago	Right

Each patient was assessed at the entry to and at the discharge from the robotic therapy session, as well as in a month follow up period. Traditional scales were used for the assessment of the impairment status and the disability of the patients. The traditional semi-quantitative scales were the Modified Ashwort Score, the FIM score (Total FIM score and separately the self-care score), and the Barthel index. Assessment of the motion ranges at two anatomic joints was made by biomechanical measurements: the CMS HS type Motion Analyzing System of zebris Medizintechnik Ltd was used [15]. Tables 4, 5, 6, and 7 show the assessment results.

The average score of shoulder adductors at admission was 1.25, while at discharge it was 1.125 which means a 10% improvement. The average score of elbow flexors at admission was 1.75, while at discharge it was 1.375 which means a 21,4% improvement. The Ashworth score of the patient #R8 has increased. When starting the therapy he had flaccid hemiparesis, as it is usual during the first weeks after the brain damage. Spasticity appeared later, as it is frequent in such cases. We suppose that without the robot-mediated physiotherapy, the increase in Ashworth score could have been higher.

Table 4. Modified Ashworth score of shoulder adductors and elbow flexors of the affected side

Patient #	**Shoulder adductors**		**Elbow flexors**	
	Admission	**Discharge**	**Admission**	**Discharge**
R1	1	1	2	1
R2	2	2	3	2
R3	0	0	1	0
R4	1	1	2	2
R5	2	2	3	2
R6	1	0	2	1
R7	3	2	3	3
R8	0	1	0	1

Table 5. Range of movement of elbow flexion-extension and pronation-supination of of the affected side

Patient #	**Elbow flexion-extension [degree]**		**Pronation-supination [degree]**	
	Admission	**Discharge**	**Admission**	**Discharge**
R1	80	87	133	137
R2	84	96	75	107
R3	106	107	120	124
R4	46	78	35	65
R5	89	99	97	97
R6	71	88	53	59
R7	29	52	47	69
R8	82	71	41	89

Table 6. FIM and self care scores (self care is a part of the total FIM score)

Patient #	Total FIM score		Self-care	
	Admission	Discharge	Admission	Discharge
R1	121	122	42	42
R2	115	122	36	42
R3	106	126	36	42
R4	115	115	36	36
R5	86	89	25	26
R6	98	106	32	35
R7	111	113	36	36
R8	103	115	29	36

Table 7. Barthel index

Patient #	Admission	Discharge
R1	100	100
R2	100	100
R3	100	100
R4	90	100
R5	70	80
R6	85	95
R7	90	95
R8	65	100

The average elbow flexion at admission was 69.5 degrees, while at discharge it was 84.75 degrees which means a 21.9% improvement. The average pronation-supination at admission was 75.1 degrees, while at discharge it was 93.4 degrees which means a 24,3% improvement.

The average FIM (Functional Independence Measure) score at admission was 106.875, while at discharge it was 113.5, which means a 6.2% improvement. The average self-care score at admission was 34, while at discharge it was 36.875, which means a 8,46% improvement. The average Barthel index at admission was 87.5, while at discharge it was 96.25, which means a 10% improvement.

The Tables show that most of our patients were not seriously disabled; we have selected them intentionally to start the first clinical trial of the REHAROB Therapeutic System with non-serious cases. Most of our patients had their brain damage years ago, nevertheless robotic physiotherapy has improved their state regarding both the level of impairment and disability. Follow up assessments proved that all patients retained their discharge statuses. To prove the clinical and economic efficiency of the robotized physiotherapy will be the objective of a second controlled trial, which is planned for next year. The most important conclusions of the current clinical trial are as follows:

1. The robotic physiotherapy system was working continuously, reliably and safely; there were no delays due to technical or other problems.
2. The patients were not afraid of the robots; they found the robotized therapy interesting and useful.
3. The physiotherapists learnt easily how to work with the robots; the user interface proved to be really user friendly.
4. Based on the physiotherapists experience smaller improvement of the system is planned such as the improvement of the safety release mechanism, the armpit support, the headrest of the couch, and the patient enabling device.

6. Conclusions

The first prototype robotic physiotherapy system has proved that standard industrial robots are suitable for robotic physiotherapy. The REHAROB Therapeutic System has some unrivalled features among the passive physiotherapy machines and robots for spastic hemiparetic patients. Such features are that REHAROB uses two synchronized robotic arms, and exercises the spastic limb over the full ranges of the 5 shoulder and shoulder girdle joints as well as the 2 elbow joints.

An attempt was made to uncover the background of the realized, and successful force control of the industrial robots. A simplified, one-dimensional model of the teaching in device was used to analyse the stability of the outer-loop, digital force control. The effect of the digital sampling and the deadtime of the robot controller is presented in the form of stability charts. These stability charts derived from the simple model confirmed the experimental results. The investigation also revealed the intricate dynamics of discrete time systems with deadtime. Results drew the attention of engineers to the destabilizing effect of digital sampling and deadtime. The current standard industrial robot controllers limit the use of these devices to physiotherapy, but with evolution of the controllers due to industrial market needs the limitations will soon disappear. In case of REHAROB the two S4C+ controllers will be replaced by the new generation of IRC5 controllers, which offers a radical improvement in the performance of outer-loop control.

All the patients included in the clinical trial have shown significant improvement in their impairment and disability indicators. Patients have found the duration, the constancy, the power, and the complexity of robotic exercises effective and calming compared with the traditional manual passive physiotherapy. As beside the robotic approach our patients received traditional physiotherapy as well, we cannot conclude with certainty that the positive changes in the status of the patients were due to the robot-mediated therapy alone. It will be the aim of the second clinical trial to prove the true clinical efficacy of the system. After minor system improvements, one year long, controlled trial is planned for 2004 and 2005 in the framework of the FIZIOROBOT project supported by the Ministry of Health, Social and Family Affairs, Hungary. The cost of the first prototype system is rather high, approx. Euro 250,000 in comparison with the average patient day costs, that is Euro 500 in Europe and Euro 1000 in the USA for large rehabilitation centres. Based on the outcome of

the second controlled trial, the REHAROB system can be optimised, and prepared for serial production and introduction to the market.

We believe that medical robotics applications must benefit from the use of mass produced and reliable industrial robots. The REHAROB Therapeutic System opens up a strong perspective of moving from taught in passive repetitive exercising to biomechanical-knowledge-based automatic passive, and later purely active upper and lower limb physiotherapy. In this respect the REHAROB Therapeutic System could cover all physiotherapy needs of a spastic hemiparetic stroke patient. In the distant future a customized physiotherapy and rehabilitation strategy for each patient can be developed and delivered automatically.

Acknowledgement. This research is sponsored by the European Commission through the IST-1999-13109 project, and by the Ministry of Health, Social and Family Affairs, Hungary through the ETT-073/2003 project and by the Hungarian National Science Foundation under grant No. OTKA T043368. Special thanks are due to the engineering and medical colleagues Mihály Jurák, Györgyi Stefanik, and Zsuzsanna Boros.

REFERENCES

1. Feher, M. and Denes, Z.: *Neuro-rehabilitation in Medical Rehabilitation.* Medicina Publisher Co., Budapest, 2005. (in Hungarian)
2. Taub, E., Miller, N. E., Novak, T. A., Cook, E. W., Fleming, W. C., Nepomuceno, C. S., Connell, J. S. and Crago J. E.: Technique to improve chronic motor deficit after stroke. *Arch Phys Med Rehabil,* **74(4)**, (1993), 347-354.
3. Lum, P., Reinkensmeyer, D., Mahoney, R., Rymer, W. Z. and Burgar, C.: Robotic devices for movement therapy after stroke: current status and challenges to clinical acceptance. *Top Stroke Rehabil.*, **8**(4), (2002), 40-53.
4. Burgar, C. G., Lum, P. S., Shor, P. C. and Van der Loos H. F. M.: Development of robots for reha-bilitation therapy: The Palo Alto VA/Stanford experience. *J. Rehabil. Res. Dev.*, **37**(6), (2000), 663-673.
5. Krebs, H. I., Volpe, B. T., Ferraro, M., Fasoli, S., Palazzolo, J., Rohrer, B., Edelstein, L. and Hogan, N.: Robot-aided neurorehabilitation: from evidence-based to science-based rehabilitation. *Top Stroke Rehabil.*, **8**(4), (2002), 54-70.
6. Amirabdollahian, F., Loureiro, R., Driessen, B. and Harwin, W.: Error Correction Movement for Machine Assisted Stroke Rehabilitation. In M. Mokhtari (ed.), *Integration of Assistive Technology in the Information Age*, IOS Press, Amsterdam, 2001, pp. 109-116.
7. Arz, G., Toth, A., Fazekas, G., Bratanov, D. and Zlatov, N.: Three-dimensional Anti-spastic Physiotherapy with the Industrial Robots of "REHAROB". *In Proc 8th Int Con Rehabilitation Robotics*, KAIST 2003, pp. 215-218.
8. Kovacs, L.∼L., Toth, A., Stepan, G., Arz, G. and Magyar, G.: Industrial Robot in a Medical Application – Back to Walk-through Programming. In D.∼T. Pham, S.∼S. Dimov, V.∼O. O'Hagan (eds.), *Advances in Manufacturing Technology – XV.*, Professional Engineering Publishing Limited, London, 2001, pp. 479-484.
9. Council Directive 93/42/EEC of 14 June 1993 concerning medical devices.
10. Hall, S. J.: *Basic Biomechanics.* WCB McGraw-Hill, 1999.

11. Pires, J. N., Ramming, J., Rauch, S. and Araújio R.: Force/Torque sensing applied to industrial robotic deburring. *Sensor Review*, **22**(3), (2002), 232-241.

12. Kuo, B. C.: *Digital Control Systems*. SRL Publishing Company, Champaign, Illinois, 1977.

13. Lakshmikantham, V. and Trigiante, D.: *Theory of Difference Equations, Numerical Methods and Applications*. Academic Press, London, 1988.

14. Stépán, G., Kollár, L.: Balancing with reflex delay. *Mathematical and Computer Modelling*, **31**, (2000), 199-205.

15. Fazekas, G., Feher, M., Kocsis, L., Stefanik, G., Boros, Z. and Jurak, M.: Application of kinematical parameters for the assessment and monitoring of central motoneuron impair-ments. *Clin. Neurosci./Ideggy. Szle.*, **55**(7-8), (2002), 268-272. (in Hungarian)